Global NEST Journal, Vol 26, No 5, 06033

Preparation of biochar-loaded nano zero-valent iron electrode material and its electrocatalytic degradation of p-nitrophenol

Qinhua Sun, Jiankun Zhang* and Linjun Zhang
School of Environmental Engineering, Xuzhou university of technology, Xuzhou, China.
Received: 09/04/2024, Accepted: 18/04/2024, Available online: 27/04/2020
*to whom all correspondence should be addressed: e-mail: zhangjiankun@xzit.edu.cn
https://doi.org/10.30955/gnj.006033

Graphical abstract

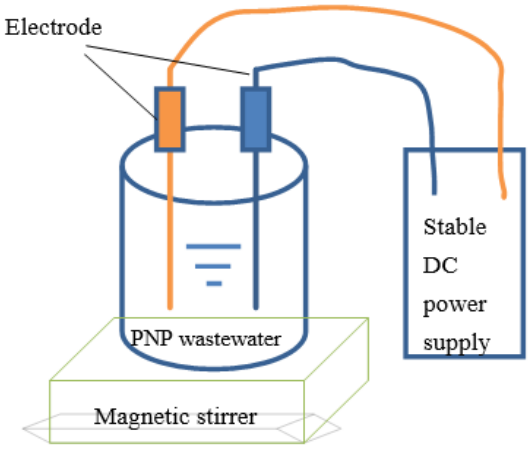

Abstract

Electrochemical treatment of wastewater containing p-nitrophenol (PNP) was carried out using a platinum electrode as an anode and biochar-loaded nano zero-valent iron material as the cathode. The prepared biochar loaded nano zero valent iron electrode materials were characterized and analyzed using SEM, XRD, and XPS. The experiment investigated the effects of current density, initial PNP concentration, electrolyte concentration, pH value, and other factors on the treatment effect of PNP. The results showed that the nZVI/BC electrode with an initial pH value of 7.0, a current density of 10mA/cm^2, and an electrolyte of 1.5g/L anhydrous sodium sulfate was the optimal condition for degrading a PNP solution with an initial concentration of 20 mg/L. The PNP removal rate within 24 hours was 81.94%. BC@nZVI electrode has good stability and reusability.

Keywords: Electrochemistry; P-nitrophenol; biochar loaded nano zero valent iron

1. Introduction

P-nitrophenol (PNP) (Dang Y *et al*. 2022; Roy D *et al*. 2021; Zhang Y *et al*. 2022; Zhang J *et al*. 2022) is a joint aromatic compound with biological solid activity and accumulation. After entering the environment, it can stay in the water for a long time and accumulate in the food chain. It is one of the 129 priority pollutants regulated by the U.S. Environmental Protection Agency (USEPA). It is also one of the priority hazardous pollutants for water pollution control in China (Tang W *et al*. 2022). Removing p-nitrophenol from water is an arduous and challenging task because their hydroxyl and nitro groups are directly connected to the benzene ring, which makes them structurally stable and nonbiodegradable, making them one of the typical organic pollutants that are difficult to degrade (Chen Y *et al*. 2023). Electrochemical methods have attracted the interest of many environmental protection workers because of their advantages, such as easy control and low treatment cost. The electrocatalytic effect is closely related to the performance of cathode materials (Qiu S *et al*. 2021; Dominguez C M *et al*. 2018), so researchers pay close attention to the removal effect of cathode materials. Some noble metal electrodes, such as Ti and Pt (Karim A V *et al*. 2021), have high electrocatalytic activity, which can directly decompose water on the electrode surface into strong oxidizing intermediate products, such as Ho, to oxidize and decompose some organic pollutants in wastewater (Zhang X *et al*. 2021). However, the high cost of noble metals Pd and Pt limits the broad application of electrocatalytic removal of PNP. Some studies have compared the catalytic reduction performance of different nonnoble metal electrodes. Nonnoble metals Sn (Liu Z *et al*. 2023), Bi (Zhang X *et al*. 2017), Fe (Kang G S *et al*. 2020), and Cu (Zhang P *et al*. 2022) are considered cathodes that have high catalytic reduction activity for PNP. To further improve the removal rate of PNP, some studies have used synthetic metal or metal oxide electrodes as the cathode of electrocatalytic reduction. In some studies, carbon nanotubes (Banks C E *et al*. 2004) and noble metal PbO_2(Zhang Z *et al*. 2021) modified graphite electrodes, significantly increasing the PNP removal rate. Suppose carbon material itself is used as the electrode. In that case, the reduction kinetics of PNP is slow, so in most studies, the carbon material is used as a nanocatalyst carrier to enhance the removal of PNP at a low cost. Common carbonaceous materials include biochar (Moradi P *et al*. 2021), activated carbon

(Yoo J M *et al*. 2022), carbon fiber (Vedrtnam A *et al*. 2019), carbon nanotubes (Yao D *et al*. 2021), graphite (Asgari G *et al*. 2020), and graphene (Ma M *et al*. 2021).

In this experiment, biochar-loaded nano zero-valent iron composite（BC@nZVI）combined with electrochemical methods, the excellent performance and low-cost electrode materials were studied. At the same time, the effects of current density, initial concentration of PNP, concentration of supporting electrolyte, initial pH value, and chloride ion concentration on the electrocatalytic reduction of PNP by composite electrode were explored, which provided theoretical support and application reference for the electrocatalytic reduction pathway and the practical application of composite electrode in PNP degradation.

2. Experimental

2.1. Materials

p-Nitrophenol (CAS:100-02-7), Ferrous sulfate (CAS:7720-78-7), Sodium borohydride (CAS:16940-66-2), Polyethylene glycol (CAS:25322-68-3), Ethyl alcohol (CAS:64-17-5), Sodium sulfate (CAS:7757-82-6), Polyvinylidene fluoride (CAS:24937-79-9), N-methyl-2-pyrrolidone (CAS:872-50-4).

All the chemical reagents used in the experiment were purchased from Sinopharm Chemical Reagent Co., Ltd. All chemicals are of analytical grade and do not need further purification during use. All solutions were prepared with deionized water.

2.2. Electrode preparation

Biochar-loaded nano zero-valent iron cathode was prepared by reducing Fe^{2+} with sodium borohydride. 4.45g $FeSO_4 \cdot 7H_2O$ and 0.5g polyethylene glycol were weighed in 400ml ethanol-water mixed solution, and 4.5g wheat straw biochar was added to the solution and stirred for 60min. Weigh the excess sodium borohydride in 30ml deionized water, use a syringe to add it to the mixed biochar and Fe^{2+}drop by drop, and keep stirring for 30min under nitrogen protection. After the complete reaction, it can stand until the solid particles are separated from the liquid. The solid particles are repeatedly cleaned with deionized water three times and then washed with anhydrous ethanol three times. Use a freeze-drying oven to dry for 30 hours until it is scorched. Take it out and put it in the tube to pass nitrogen for 10 minutes to remove the oxygen. Store it in cold storage at 4 °C.

Preparation of biochar loaded nano zero-valent iron cathode: Weigh 0.1g polyvinylidene fluoride (PVDF) in an appropriate amount of N-methyl-2-pyrrolidone (NMP), stir to dissolve it fully, add 0.1g acetylene black, stir to thoroughly mix it, weigh 0.8g biochar loaded nano zero-valent iron composite, simply stir the mixture to a uniform paste, and evenly scrape the above mixture on the graphene matrix, Put it in a vacuum drying oven and dry it at 60 ℃ overnight. After drying, the biochar-loaded nano zero-valent iron cathode was obtained by pressing the tablet under 20MPa pressure with a powder tablet press marked BC@nZVI.

2.3. Electrode characterization

Characterization of biochar loaded nano zero-valent iron by scanning electron microscopy (Regulus 8100; Hitachi Japan) （BC@nZVI） The surface morphology of the material; Determine the crystal structure of the material using an X-ray diffractometer (D8 Advance; Brooke Germany) and analyze its corresponding X-ray diffraction peaks BC@nZVI Chemical composition and composition of materials, scanning range 2θ 10°~60°; Analysis by X-ray photoelectron spectroscopy (ESCALAB 250Xi; Thermo Fisher Scientific, USA) BC@nZVI The composition and chemical state of chemical elements.

2.4. Electrochemical reactor

The experimental device is shown in Figure 1. A 1000ml five-port unsealed electrolytic cell is used as the reactor. Two fixed electrode holes are selected on the reactor cover to maintain a distance between the anode and cathode. The high-purity platinum anode is purchased from Shanghai Leton Industrial Co., Ltd. The cathode is a self-made biochar-loaded nano zero-valent iron cathode, and the constant current is supplied by utp3313tfl-ii DC regulated power supply; the reactor is placed on a magnetic stirrer for continuous stirring to make the solution concentration uniform during the reaction process.

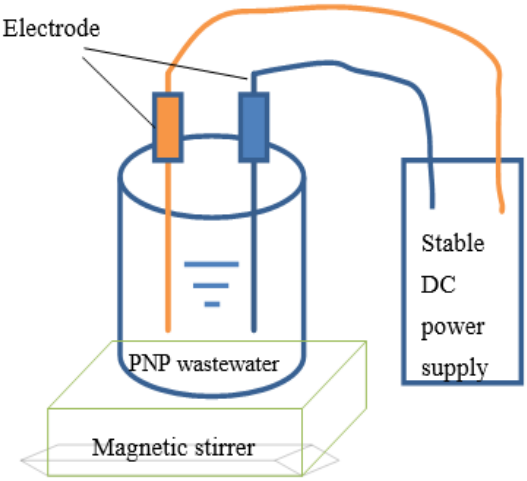

Figure 1. Experimental apparatus

2.5. Measurements

The results showed that a 1 cm thick quartz cuvette was used at the wavelength of 317 nm, and the UV spectrophotometry (HJ/T346-2007) was the most suitable method to detect p-nitrophenol in the solution; PH is measured by PHSJ-6L pH meter. The main parameters in the experiment are calculated as follows:

The PNP removal rate is calculated as follows:

$$R_{PNP}(\%) = \frac{[PNP]_0 - [PNP]_t}{[PNP]_0} \times 100\%$$

In the formula, $[PNP]_0$is the initial concentration of PNP; $[PNP]_t$ is the PNP concentration measured after the reaction reaches time t.

3. Results and discussion

3.1. Surface morphology and crystal structure

3.1.1. Surface morphology analysis

Figure 2 shows biochar-loaded nano zero-valent iron (BC@nZVI). Scanning electron microscopy (SEM) and EDS spectra were obtained. After loading nano iron, black particles on the biochar surface have a relatively uniform particle size. The SEM analysis results of the biochar loaded with nano iron show no accumulation of nano iron loaded onto the biochar, which increases the activity of the nano iron material. By combining it with biochar, the efficiency of pollution removal is improved. In the EDS spectrum, carbon, oxygen, and iron were detected in the BC@nZVI material, demonstrating the successful loading of nano-zero-valent iron onto biochar carriers.

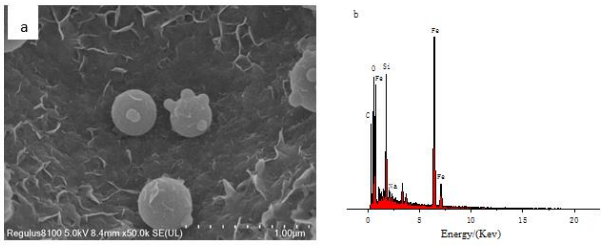

Figure 2. SEM and EDS spectra of BC@nZVI electrode materials, a: SEM, b: EDS

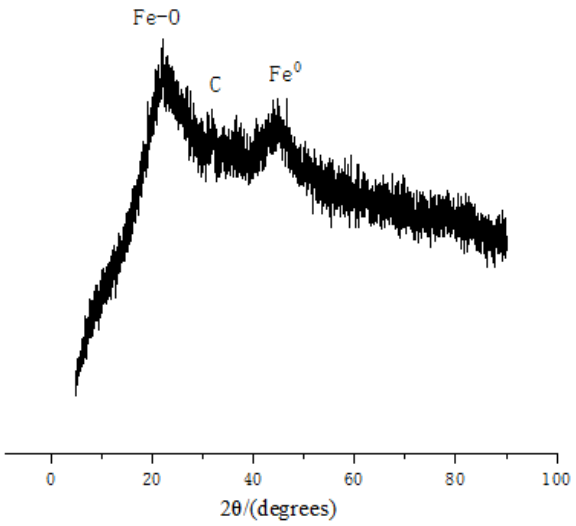

Figure 3. BC@nZVI XRD patterns of electrode materials

3.1.2. Crystal structure analysis

BC@nZVI, The XRD diffraction pattern of the material is shown in Figure 3, BC@nZVI. The material exhibits a Fe^0 characteristic peak at 2θ=42–44°(Bakdemir S A *et al*. 2023), but the diffraction peak was relatively weak in width and diffused, while the diffraction peak intensity of nano zero-valent iron was high and sharp(Danish M *et al*. 2017). This indicates that nano zero-valent iron adheres to the surface of biochar or enters its internal pores, but the amount of nano zero-valent iron is much smaller than that of individual nano zero-valent iron. Some small peaks at around 2 θ = 35° and 26° are iron oxides, indicating that some zero-valent iron loaded on biochar has been oxidized into Fe_2O_3, Fe_3O_4, and FeOOH. Biochar-loaded nano zero-valent iron has a diffraction peak of amorphous carbon that appeared around 2θ = 22°, First, the nano-zero-valent iron material is loaded onto the surface of the biochar. Secondly, the stirring effect during the loading process caused some biochar pores to collapse (Min L *et al*. 2020).

3.1.3. Elemental analysis

BC@nZVI, The XPS spectrum of the electrode material is shown in Figure 4. Figure 4 (a) shows the complete spectrum scanning of the material. They are combined with the detection results in Figures 4 (b), (c), and (d). Characteristic peaks such as C, Fe, O, and Na can be observed, indicating that the material surface mainly comprises these four elements. Figure 4 (b) shows the spectrum of Fe2p XPS, with two significant peaks appearing at 711.67eV and 724.87eV, respectively, mainly the oxides of divalent iron and trivalent iron (Saha S K *et al*. 2023). This should be made for BC@nZVI Caused by the oxidation of zero-valent iron in the air. Figure 4 (c) shows the spectrum of O1s XPS, with the highest peak at 532.7eV, mainly due to the formation of Fe_2O_3. The spectrum ranges from 529.5eV to 535.5eV, mainly due to the binding energy of O^{2-}, OH, and adsorbed water molecules (Zhou Z *et al*. 2021).

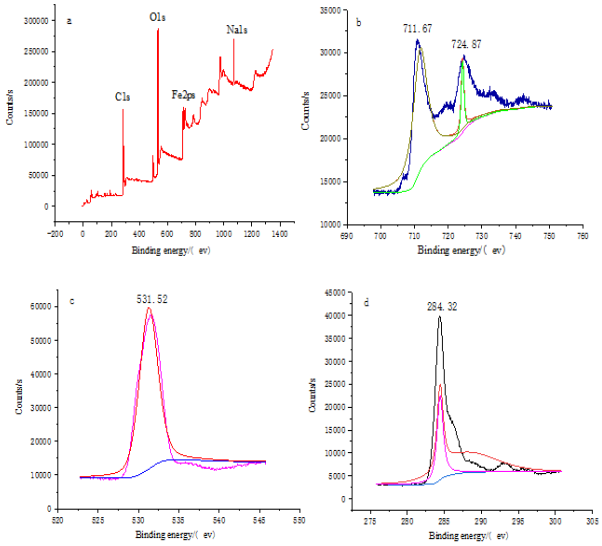

Figure 4. XPS Atlas of BC@nZVI, a: BC@nZVI full scan, b: Fe, c: O, d: C

3.2. Degradation of PNP by Different Electrode Systems

Using a high-purity platinum plate electrode as an anode, the comparison of nZVI electrode, BC electrode, foam graphene substrate BC@nZVI the electrode is the cathode, electrocatalysis the degradation of PNP. Using an electrolytic cell as the reactor, 1.5g/L Na_2SO_4 was added to a PNP solution with an initial concentration of 20mg/L as the supporting electrolyte. The pH of the solution in the reactor was adjusted to 7, and the current density was maintained at 10mA/cm^2. The DC stabilized power supply stabilized the current at 0.04A, and the reaction was carried out at room temperature for 24 hours. A specific time was set to sample and measure the absorbance of the solution, and the removal rate of PNP was calculated. The results are shown in Figure 5.

From the figure, it can be seen that when graphene substrate and BC electrode are used as cathodes, the PNP removal rate is meager; that is, the decrease in PNP concentration is minimal, with PNP concentration decreasing from 20mg/L to 12.8 mg/L and 15.52 mg/L, respectively. When BC@nZVI, The PNP concentration of the electrode dropped from 20mg/L to 19.21mg/L without electricity, and the PNP removal rate was only 3.95%. Therefore, the removal effect of PNP by nano zero valent iron modified biochar electrode is minimal without electricity. Simultaneously using nZVI electrodes and BC@nZVI When the electrode is a cathode, the PNP removal rate is significantly lower than the first two electrodes; that is, the PNP concentration decreases significantly, and the PNP removal rate BC@nZVI The electrode is greater than the nZVI electrode, and from the experiment of influencing factors, it can be seen that the concentration of PNP changes significantly in the first ten hours, and tends to flatten out in the last ten hours, which is different from the approximate linear decrease of PNP concentration when BC electrode and graphene substrate are used as cathodes; It is also worth noting that after the reaction BC@nZVI There were no significant changes such as falling or fracture on the surface of the electrode, while there was a considerable oxide layer on the surface of the nzVI electrode. The Fe^0 content in the nzVI electrode differed from that of the BC@nZVI. The removal rates of PNP are significantly different, indicating that BC can effectively disperse nZVI, reduce the aggregation of nZVI, and make PNP more effectively contact the active sites of nZVI. At the same time, the porous structure of biochar can better solve the problem of easy oxidation of nZVI.

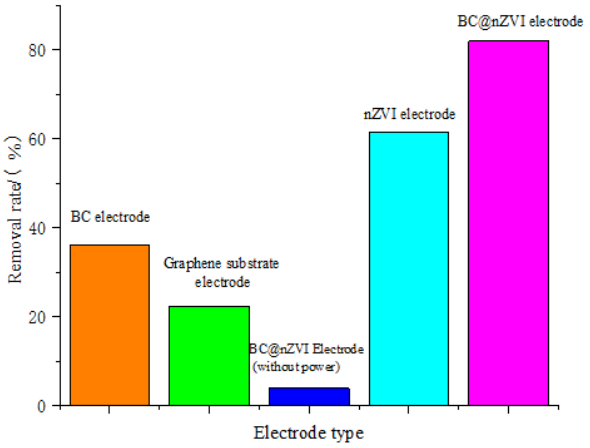

Figure 5. PNP removal efficiency of different cathode systems

3.3. Influence of current density

By changing the output current of the DC-regulated power supply to 0.02A, 0.04A, 0.06A, 0.08A, and 0.18A and maintaining the current density during the electrocatalytic process to 5 mA/cm^2, 10 mA/cm^2, 15 mA/cm^2, 20 mA/cm^2, and 45 mA/cm^2 respectively, the effect of different current density on the removal of PNP was studied. The initial concentration of PNP is 20 g/L, the initial pH in the reactor is neutral, 1.5 g/L Na_2SO_4 is added as the supporting electrolyte, the reaction is carried out at room temperature for 24 hours, the disposable sampler is set for a specific time to sample, and the absorbance of PNP solution is detected after filtering with a 0.45 μm filter head. The test results are shown in Figure 6.

From the graph, it can be seen that the overall PNP removal rate increases with the increase in current density. When the current density is 5mA/cm^2, 10mA/cm^2, 15mA/cm^2, 20mA/cm^2, and 45mA/cm^2, the PNP removal rates are 57.61%, 83.76%, 70.23%, 80.19%, and 93.37%, respectively. The PNP removal rate significantly increases when the current density increases from 5mA/cm^2 to 10mA/cm^2. When the current density increases to 45mA/cm^2, The removal rate of PNP rapidly increases to 93.37%, which is because when the current density is too high, a large amount of active hydrogen generated by the cathode can indirectly reduce part of PNP. At the same time, the increase of applied current is conducive to Electron transfer in PNP solution and increases the number of electrons, thus accelerating the degradation of PNP. However, increasing the current density can effectively improve the PNP removal rate, but as the current density gradually increases, the current efficiency significantly decreases, and energy consumption continues to increase. Based on factors such as PNP removal rate, current efficiency, and energy consumption, a current density of 10mA/cm^2 was used for exploration in subsequent experiments.

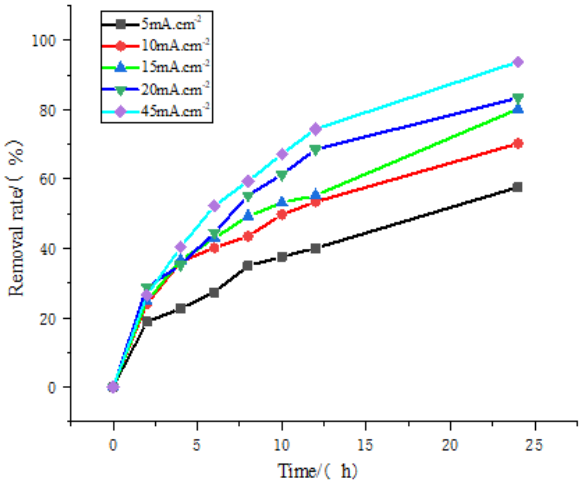

Figure 6. PNP removal rate under different current densities

3.4. Effect of initial PNP concentration

The initial concentrations of PNP prepared were 10mg/L, 20mg/L, 30mg/L, 40mg/L, and 60mg/L, respectively, to investigate the effect of initial PNP concentration on the removal rate of electrocatalytic PNP. Use the DC stabilized power supply to maintain the current density of 10mA/cm^2, add 1.5g/L anhydrous sodium sulfate as the supporting electrolyte, adjust the pH of the solution in the reactor to neutral, use the Magnetic stirrer to make the solution more uniform, react at room temperature for 24h, set a specific time for sampling, filter the solution with 0.45 μm filter head and detect the absorbance of the resolution, to calculate the solution concentration and removal rate. The results are shown in Figure 7.

When the initial PNP concentrations were 10mg/L, 20mg/L, 30mg/L, 40mg/L, and 60mg/L, the removal rates of PNP were 88.9613%, 81.9364%, 80.8492%, 83.7553%,

and 78.5772%, respectively. It can be seen that the overall PNP removal rate decreased with the increase of the initial PNP concentration. When the initial PNP concentration was between 20mg/L and 60mg/L, although the overall removal rate decreased, the decrease was not significant. This indicates that under the set experimental conditions, BC@nZVI the electrode can solve the problem of removing phenolic pollutants such as PNP from sewage in the most commonly polluted areas. Although the PNP removal rate decreases with the increase of initial PNP concentration, the total amount of PNP removal increases because, at the same current density, lower concentrations of PNP can fully adsorb on the BC@nZVI On the electrode surface because of the low concentration of PNP, the Active site of nZVI is relatively sufficient. However, as the concentration of PNP in the solution increases, the mass transfer of PNP itself will be limited, thus slowing down the reduction rate of PNP. When PNP reaches the cathode surface, too much PNP will form adsorption competition on the cathode surface and block the Active site, decreasing the reaction rate. That is, the removal rate of PNP will decline.

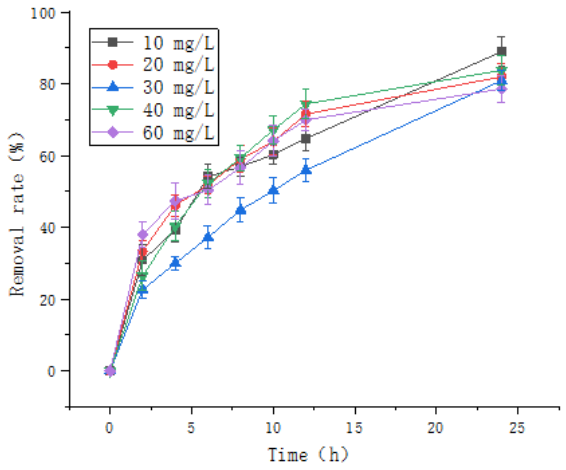

Figure 7. Effect of initial PNP concentration on removal rate

3.5. Effect of initial pH

By dropping 0.5mol/L sodium hydroxide solution and dilute hydrochloric acid solution into PNP solution, the initial pH of PNP solution is adjusted to 5.0, 6.0, 7.0, 8.0 and 9.0, respectively, to explore the influence of different initial pH on PNP removal rate. Add 1.5g/L anhydrous sodium sulfate into the reactor solution as the supporting electrolyte, use the DC stabilized power supply to maintain the current density of 10mA/cm^2, place the reactor on the Magnetic stirrer, maintain the constant speed of the Magnetic stirrer, react at room temperature for 24 hours, set a specific time for sampling, filter through 0.45 μm filter head, measure the absorbance, and calculate the PNP removal rate. The experimental results are shown in Figure 8.

It can be seen from Figure 8 that the PNP removal rate first increases and then decreases with the initial pH value. When the initial pH value of the solution is 5, 6, 7, 8, and 9, the PNP removal rate is 86.40%, 70.78%, 83.76%, 86.61%, and 81.94%, respectively. Some researchers pointed out that under acidic conditions, the PNP removal efficiency of Biochar loaded with nano zero valent iron is higher because, at a lower pH value, the solution contains a large amount of H+, which is more conducive to the reduction of PNP; However, in electrochemical experiments, not only reduction reactions occur at the cathode, but also hydrogen evolution reactions occur at the cathode. Acidic conditions are conducive to hydrogen evolution reactions, as H+ consumes some electrons to produce H_2, but the cathode can only provide limited electrons at any time. Therefore, the occurrence of hydrogen evolution reactions will inevitably delay the reduction of some PNP, thereby reducing the PNP removal rate.

On the other hand, if the solution is alkaline, the hydrogen evolution reaction is inhibited. Still, the H+ in the solution is significantly reduced, so the indirect reduction effect of PNP is affected dramatically. In addition, 24 hours after the reaction, the pH value of the solution increased from 5.0, 6.0, 7.0, 8.0, 9.0 to 9.58, 9.67, 9.78, 9.92, and 10.34, respectively, because a large number of negatively charged ions would be lost in the process of electrocatalytic reduction of PNP. According to the Conservation law, many negatively charged ions must be formed. The electrocatalytic reduction of PNP follows the principle of electroneutrality, reducing negative charges in the reaction and requiring OH- to stabilize the response.

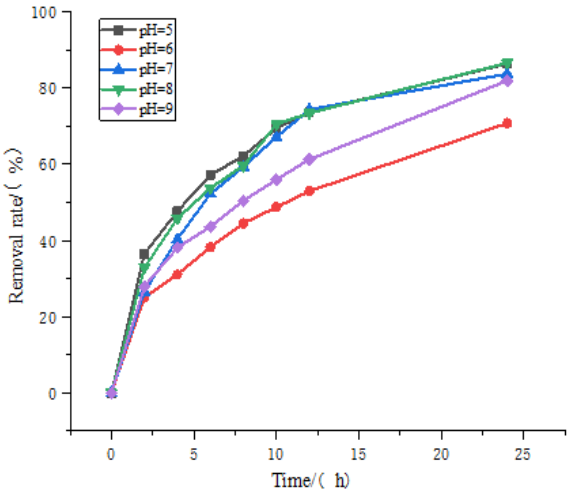

Figure 8. PNP removal rates under different initial pH values

3.6. Effect of electrolyte concentration

By adding anhydrous sodium sulfate of different masses (0.1 g, 0.5 g, 1.0 g, 1.5 g, 2.0 g, 3.0 g) into the PNP solution, adjust the electrolyte concentration in the reactor to 0.1g/L, 0.5 g/L, 1.0 g/L, 1.5 g/L, 2.0 g/L, 3.0 g/L respectively, and explore the influence of different supporting electrolyte concentrations on the removal rate of PNP. The initial concentration of PNP is 20mg/L, the initial pH in the reactor is adjusted to 7, the current density is maintained at 10mA/cm^2 through a DC-stabilized power supply, and the reactor reacts at room temperature for 24 hours. Set a time for sampling, filter with a 0.45 μm filter head, and measure the absorbance to calculate the PNP removal rate. The results are shown in Figure 9.

From the figure, it can be seen that when the supporting electrolyte concentrations are 0.1 g/L, 0.5 g/L, 1.0 g/L, 1.5 g/L, 2.0 g/L, and 3.0 g/L, the PNP concentration degrades from 20 g/L to 10.12 g/L, 6.44 g/L, 3.71 g/L, 3.25 g/L, 2.94 g/L, and 3.67 g/L, respectively. After calculation, the PNP removal rate can be obtained under different electrolyte concentration conditions. When the electrolyte concentration is 0.1 g/L, the PNP removal rate is the lowest, below 50%. This is because when the electrolyte concentration in the reactor is too low, the conductivity is insufficient to support electron transfer in the electrocatalytic process. Increasing the electrolyte concentration to 0.5 g/L can significantly improve the removal rate of PNP. Because adding Na_2SO_4 ions increases the conductivity of the solution itself, thereby increasing the conductivity. This is equivalent to an increase in the current of the reaction system at the same voltage, thereby effectively improving the removal rate of PNP. When the electrolyte concentration increases from 0.5 g/L to 2.0 g/L, the removal rate of PNP increases slightly, but when the electrolyte concentration increases to 3.0 g/L, the removal rate decreases compared with the result of 2.0 g/L. This is because although the increase of electrolyte concentration will improve the removal rate of nitrate nitrogen when the system conductivity reaches a certain level, the excess SO_4^{2-} will compete with other anions to adsorb onto the cathode, and SO_4^{2-} occupies the Active site, Reduced the contact area between PNP and the active site, affecting the removal rate of PNP.

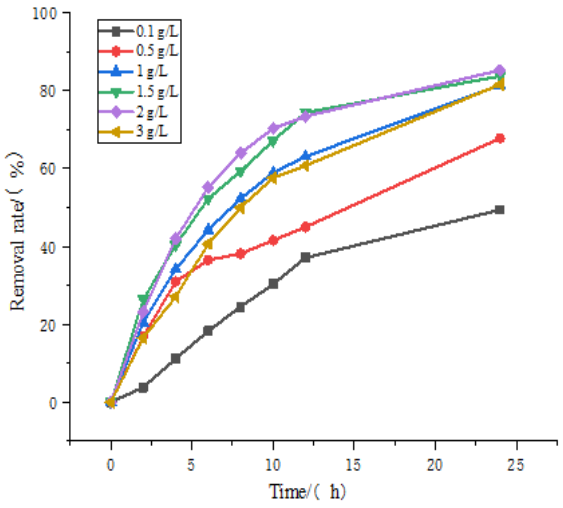

Figure 9. PNP removal rate under different electrolyte concentrations

3.7. BC@nZVI Reuse performance of electrodes

The determination of whether electrodes can be used in actual production mainly depends on the stability and reusability of the electrodes. The above electrocatalytic experiment has proven that the experimental preparation BC@nZVI the electrode has a good removal effect on PNP. Under the optimal conditions of the above influencing factors, five electrocatalytic reductions of PNP were carried out. At the end of each cycle, a disposable sampler was used to sample the PNP in the solution. After filtering with a 0.45 μm filter head, the absorbance was measured, and the PNP removal rate was calculated. The results are shown in Figure 10.

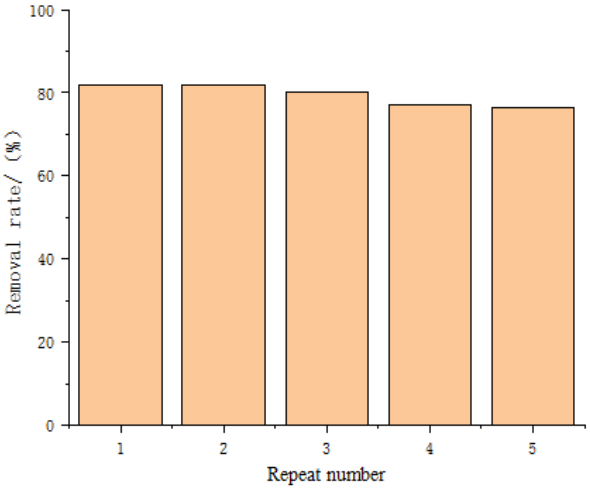

Figure 10. PNP removal rate under different reuse times

The removal rate of PNP by the electrode reached 81.94% for the first time, 82.01% after the second time, and 85.35% after five experimental cycles. After five cycles of experiments, BC@nZVI the decrease in electrode removal rate is minimal. After each experiment, the leaching amount of iron ions was measured, and it was found that the loss of iron ions was almost zero, indicating that BC@nZVI the electrode can be reused. After calculation, it can be concluded that the current efficiency remained around 38% in the five electrocatalytic experiments. After five cycles, BC@nZVI No cracks or layering were observed on the surface of the electrode, which also proves that BC@nZVI has the reliable stability of the electrode. The above experimental results indicate that BC@nZVI Electrodes are stable and reusable and should be applied in large-scale production.

4. Conclusion

(1) Nano zero-valent iron-modified biochar materials were prepared using the liquid phase reduction method, and BC@nZVI Electrodes prepared graphene-based biochar materials. The electrode materials prepared were characterized and analyzed using SEM, XRD, and XPS, and biochar effectively reduced the aggregation and oxidation of nZVI. BC@nZVI the electrode exhibits good electrocatalytic removal of PNP. The optimal condition for testing a PNP solution with an initial concentration of 20 mg/L is an nZVI/BC electrode with an initial pH value of 7.0 and a current density of 10mA/cm^2, and an electrolyte of 1.5g/L anhydrous sodium sulfate. The PNP removal rate within 24 hours is 81.94%.

(2) The nzVI/BC electrode has good stability and reusability. After five cycles of experiments, BC@nZVI the removal rate of PNP by the electrode remains almost unchanged.

Acknowledgements

The study was financially supported by the significant natural science research projects of colleges and universities in Jiangsu province(21KJA610006), supported by the Xuzhou Key Research and Development Plan (Social Development) Project (KC22302).

References

Asgari G., Seidmohammadi A., Faradmal J., Esrafili A., Sepehr M.N. and Jafarinia M. (2020). Optimization of synthesis a new composite of nano-MgO, CNT and Graphite as a catalyst in heterogeneous catalytic ozonation for the treatment of pesticide-laden wastewater. *Journal of Water Process Engineering*, **33**, 101082.

Bakdemir S.A., Özkan D., Türküz C. and Salman S. (2023). Wear performance under dry and lubricated conditions of duplex treatment TiN/TiCrN coatings deposited with different numbers of CrN interlayers on steel substrates. *Wear*, **526**, 204931.

Banks C.E., Moore R.R., Davies T.J. and Compton R.G. (2004). Investigation of modified basal plane pyrolytic graphite electrodes: definitive evidence for the electrocatalytic properties of the ends of carbon nanotubes. *Chemical Communications*, (**16**), 1804–1805.

Chen Y., Zhang M., Chen T., Zhang G., Xu H., Sun H. and Zhang L. (2023). Facile fabrication of rGO/PPy/nZVI catalytic microreactor for ultrafast removal of p-nitrophenol from water. *Applied Catalysis B: Environmental*, **324**, 122270.

Dang Y., Bai Y., Zhang Y., Yang X., Sun X. and Yu S. *et al*. (2022). Tannic acid reinforced electro-fenton system based on go-fe3o4/nf cathode for the efficient catalytic degradation of pnp. *Chemosphere*, **289**, 133046.

Danish M., Gu X., Lu S., Ahmad A., Naqvi M., Farooq U., Xue Y. *et al*. (2017). Efficient transformation of trichloroethylene activated through sodium percarbonate using heterogeneous zeolite supported nano zero valent iron-copper bimetallic composite. *Chemical engineering journal*, **308**, 396–407.

Dominguez C.M., Oturan N., Romero A., Santos A. and Oturan M.A. (2018). Lindane degradation by electrooxidation process: effect of electrode materials on oxidation and mineralization kinetics. *Water research*, **135**, 220–230.

Kang G.S., Jang J.H., Son S.Y., Lee C.H., Lee Y.K., Lee D.C. and Joh H.I. (2020). Fe-based non-noble metal catalysts with dual active sites of nanosized metal carbide and single-atomic species for oxygen reduction reaction. *Journal of Materials Chemistry A*, **8**(42), 22379–22388.

Karim A.V., Nidheesh P.V. and Oturan M.A. (2021). Boron-doped diamond electrodes for the mineralization of organic pollutants in the real wastewater. *Current Opinion in Electrochemistry*, **30**, 100855.

Liu Z., Jiang Y., Zhang Z., Wang X., Liu K., Qiao Z. and Gao C. (2023). Synthesis of noble/non-noble metal alloy nanostructures via an active-hydrogen-involved interfacial reduction strategy. *Nature Synthesis*, **2**(2), 119–128.

Ma M., Li H., Xiong Y. and Dong F. (2021). Rational design, synthesis, and application of silica/graphene-based nanocomposite: A review. *Materials & Design*, **198**: 109367.

Min L., Zhongsheng Z., Zhe L. and Haitao W. (2020). Removal of nitrogen and phosphorus pollutants from water by FeCl3-impregnated biochar. *Ecological Engineering*, **149**, 105792.

Moradi P. and Hajjami M. (2021). Magnetization of biochar nanoparticles as a novel support for fabrication of organo nickel as a selective, reusable and magnetic nanocatalyst in organic reactions. *New Journal of Chemistry*, **45**(6), 2981–2994.

Qiu S., Guo Z., Naz F., Yang Z. and Yu C. (2021). An overview in the development of cathode materials for the improvement in power generation of microbial fuel cells. *Bioelectrochemistry*, **141**, 107834.

Roy D., Neogi S. and De S. (2021). Highly efficient reduction of p-Nitrophenol by sodium borohydride over binary ZIF-67/g-C3N4 heterojunction catalyst. *Journal of Environmental Chemical Engineering*, **9**(6), 106677.

Saha S.K., Takano T., Fushimi K., Sakairi M. and Saito R. (2023). Passivity of iron surface in curing cement paste environment investigated by electrochemical impedance spectroscopy and surface characterization techniques. *Surfaces and Interfaces*, **36**, 102549.

Tang W., Pei Y., Zheng H., Zhao Y., Shu L. and Zhang H. (2022). Twenty years of China's water pollution control: Experiences and challenges. *Chemosphere*, **295**, 133875.

Vedrtnam A. and Sharma S.P. (2019). Study on the performance of different nano-species used for surface modification of carbon fiber for interface strengthening. Composites Part A: *Applied Science and Manufacturing*, **125**, 105509.

Yao D., Yang H., Hu Q., Chen Y., Chen H. and Williams P.T. (2021). Carbon nanotubes from post-consumer waste plastics: Investigations into catalyst metal and support material characteristics. *Applied Catalysis B: Environmental*, **280**, 119413.

Yoo J.M., Shin H., Chung D.Y. and Sung Y.E. (2022). Carbon shell on active nanocatalyst for stable electrocatalysis. *Accounts of Chemical Research*, 55(9), 1278–1289.

Zhang J., Chen L. and Zhang X. (2022). Removal of P-nitrophenol by nano zero valent iron-cobalt and activated persulfate supported onto activated carbon. *Water*, **14**(9): 1387.

Zhang P., Xiong J., Yu Q., Li Y., Wei Y., Zhao Z. and Liu J. (2022). Efficient purification of auto-exhaust carbon particles over non-noble metals (Fe, Co, Cu) decorated hexagonal NiO nanosheets. *Fuel*, **330**, 125662.

Zhang X., Wang Y., Liu C., Yu Y., Lu S. and Zhang B. (2021). Recent advances in non-noble metal electrocatalysts for nitrate reduction. *Chemical Engineering Journal*, **403**, 126269.

Zhang X., Yu S., Liu Y., Zhang Q. and Zhou Y. (2017). Photoreduction of non-noble metal Bi on the surface of Bi2WO6 for enhanced visible light photocatalysis. *Applied Surface Science*, **396**, 652–658.

Zhang Y., Yang S., Wei L., Zhao X. and Lu X. (2024). Degradation characteristics of p-nitrophenol and atenolol by carbon nitride modified by graphene quantum dots. *Environmental Technology*, **45**(5), 972–987.

Zhang Z., Yi G., Li P., Wang X., Wang X., Zhang C. and Zhang Y. (2021). Recent progress in engineering approach towards the design of PbO2-based electrodes for the anodic oxidation of organic pollutants. *Journal of Water Process Engineering*, **42**, 102173.

Zhou Z., Shen Z., Song C., Li M., Li H. and Zhan S. (2021). Boosting the activation of molecular oxygen and the degradation of tetracycline over high loading Ag single atomic catalyst. *Water Research*, **201**, 117314.